PRISMS-Plasticity

Crystal Plasticity

Crystal plasticity constitutive model

Classical single-crystal plasticity theory is used to model the deformation within each grain. The theory is based on the notion that plastic flow takes place through slip on prescribed slip systems. For a material with $\alpha = 1, \ldots, N$ slip systems defined by ortho-normal vector pairs $(\boldsymbol{m}_0^\alpha, \boldsymbol{n}_0^\alpha)$ denoting the slip direction and slip plane normal respectively at time $t = 0$, the constitutive equations relate the following basic fields (all quantities expressed in crystal lattice coordinate frame): the deformation gradient defined with respect to the initial undeformed crystal $\boldsymbol{F}$ which can be decomposed into elastic and plastic parts as $\boldsymbol{F} = \boldsymbol{F}^e\ \boldsymbol{F}^p$ (with $\det(\boldsymbol{F}^p) = 1$), the Cauchy stress $\boldsymbol{\sigma}$ and the slip resistances $s^\alpha > 0$. In the constitutive equations to be defined below, the Green elastic strain measure $\bar{\boldsymbol{E}}^e = \frac{1}{2}\left(\boldsymbol{F}^{eT}\boldsymbol{F}^e - \boldsymbol{I}\right)$ defined on the relaxed configuration (plastically deformed, unstressed configuration) is utilized. The conjugate stress measure is then defined as $\bar{\boldsymbol{T}} = \det(\boldsymbol{F}^e)(\boldsymbol{F}^e)^{-1}\boldsymbol{\sigma}(\boldsymbol{F}^e)^{-T}$. Kinematics of single crystal slip is illustrated in Fig. 1.

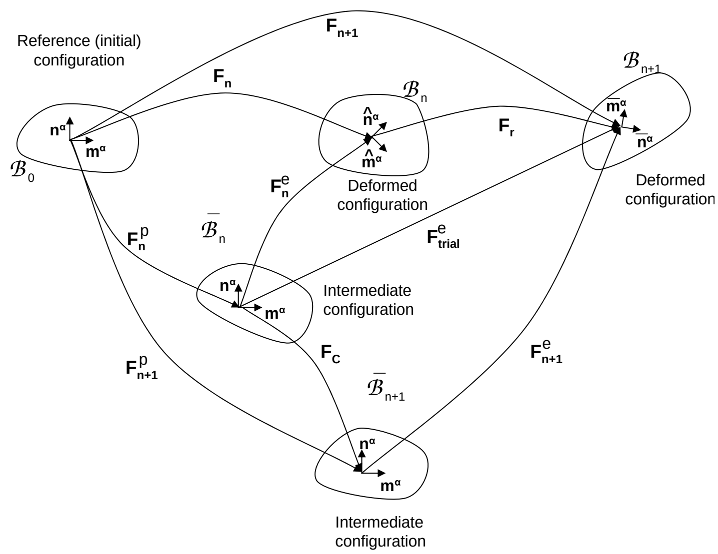

Figure 1: Schematic of the various material configurations, for a single crystal, used in the integration of the constitutive model. The slip systems ($\boldsymbol{m}^\alpha, \boldsymbol{n}^\alpha$ are known on the reference (initial) configuration. Also, $\hat{\boldsymbol{m}}^\alpha$, $\bar{\boldsymbol{m}}^\alpha$ are the slip directions (different from $\boldsymbol{m}^\alpha$ because of crystal re-orientation) in the deformed configurations $\mathcal{B}_n$ and $\mathcal{B}_{n+1}$, respectively.

The constitutive relation, for stress, is given by $\bar{\boldsymbol{T}} = \boldsymbol{\mathcal{L}}^e\left[\bar{\boldsymbol{E}}^e\right]$ where $\boldsymbol{\mathcal{L}}^e$ is the fourth-order anisotropic elasticity tensor. It is assumed that deformation takes place through dislocation glide and the evolution of the plastic velocity gradient is given by:

$$\boldsymbol{L}^p = \dot{\boldsymbol{F}}^p(\boldsymbol{F}^p)^{-1} = \sum_\alpha \dot{\gamma}^\alpha \boldsymbol{S}_0^\alpha \mathrm{sign}(\tau^\alpha) \tag{1}$$

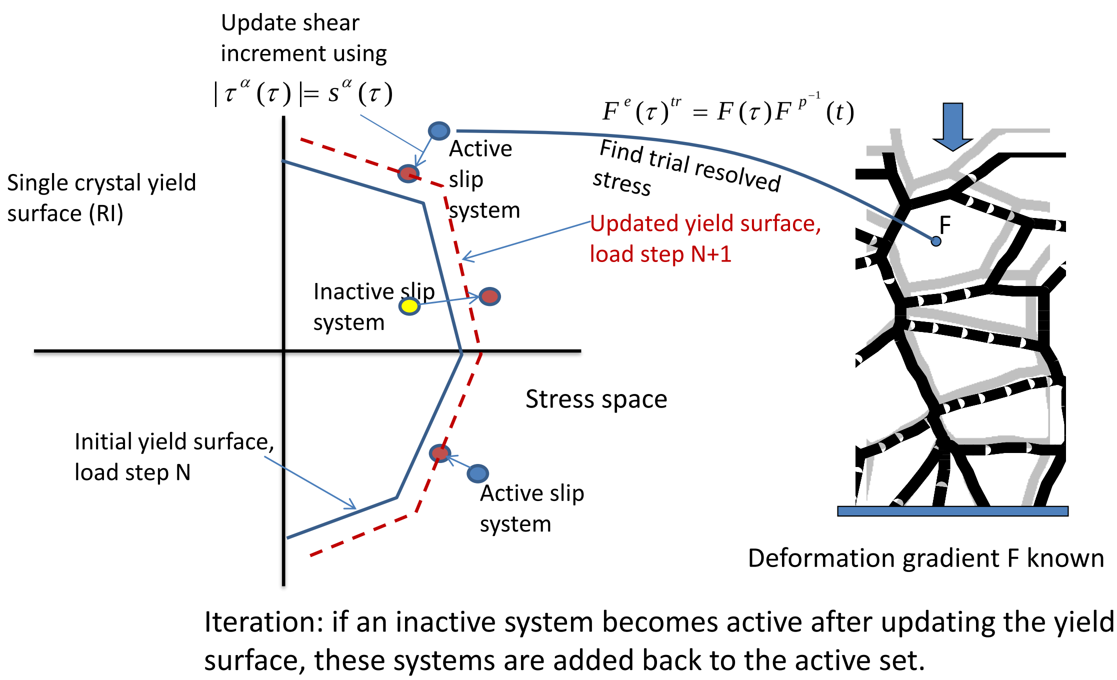

Figure 2: Schematic of the active slip systems and computation of the updated yield surface. The iterative algorithm ensures that that all the slip systems lie on or inside the yield surface.

where $\boldsymbol{S}_0^{\alpha} = \boldsymbol{m}_0^{\alpha} \otimes \boldsymbol{n}_0^{\alpha}$ is the Schmid tensor and $\dot{\gamma}^{\alpha}$ is the plastic shearing rate on the α^{th} slip system.

The resolved stress on the α^{th} slip system is given by $\tau^{\alpha} = (\boldsymbol{C}^e\ \bar{\boldsymbol{T}}) \cdot \boldsymbol{S}_0^{\alpha}$. This follows from [1] that the plastic power per unit volume in this configuration may be defined by $\dot{\omega} = (\boldsymbol{C}^e\ \bar{\boldsymbol{T}}) \cdot \boldsymbol{L_p}$ with $\boldsymbol{C}^e = \boldsymbol{F}^{eT}\boldsymbol{F}^e$. The resolved shear stress is defined through the relation $\dot{\omega} = \sum_{\alpha} \tau^{\alpha}\dot{\gamma}^{\alpha}$.

A rate independent algorithm is employed to solve the single crystal problem [2]. The resolved shear stress τ^{α} is taken to attain a critical value s^{α} (the slip system resistance) on the systems where slip occurs. These active systems have a plastic shearing rate $\dot{\gamma}^{\alpha} > 0$, where $\dot{\gamma}^{\alpha}$ is assumed to be constant during the time step. There is no plastic shearing rate, i.e., $\dot{\gamma}^{\alpha} = 0$ on inactive slip systems where the resolved shear stress does not exceed s^{α}. The evolution of slip system resistance given by the following expression:

$$\dot{s}^{\alpha}(t) = \sum_{\beta} h^{\alpha\beta}(t)\dot{\gamma}^{\beta}(t), \quad s^{\alpha}(0) = \tau_0^{\alpha} \tag{2}$$

where

$$h^{\alpha\beta}(t) = \begin{cases} h_o^\beta \left(1 - \frac{s^\beta(t)}{s_s^\beta}\right)^a, & \text{if } \alpha = \beta, \quad \text{or for coplanar systems} \\ h_o^\beta q \left(1 - \frac{s^\beta(t)}{s_s^\beta}\right)^a, & \text{otherwise.} \end{cases}$$

with h_o^β indicating the self-hardening rate and the parameter q, with values in the range 1 < q < 1.4, representing a latent-hardening parameter. Subsequently, the plastic part of the deformation gradient is updated using Eq. (1), the elastic part computed from $\boldsymbol{F} = \boldsymbol{F}^e\ \boldsymbol{F}^p$. The conjugate stress measure, $\bar{\boldsymbol{T}}$ is then computed from $\bar{\boldsymbol{T}} = \boldsymbol{\mathcal{L}}^e\left[\bar{\boldsymbol{E}}^e\right]$ and converted to Cauchy stress and the Piola-Kirchhoff-I stress, $\boldsymbol{P} = (\det\boldsymbol{F})\boldsymbol{\sigma}\boldsymbol{F}^{-T}$ for further use. The slip resistances are also updated at the end of the time step using Eq. 2 .

The rate independent model is used to find the PKI stress and tangent modulus for getting the finite element nodal displacements. The deformation gradient can be decomposed into elastic and plastic parts as follows,

$$\boldsymbol{F} = \boldsymbol{F}^e\ \boldsymbol{F}^p \tag{3}$$

where $\boldsymbol{F}^e$ is the elastic deformation gradient, while $\boldsymbol{F}^p$ is plastic deformation gradient with $\det(\boldsymbol{F}^p) = 1$. The plastic flow rule is given by the sum of strain rate over all slip systems,

$$\dot{\boldsymbol{F}}^p(\boldsymbol{F}^p)^{-1} \;=\; \sum_\alpha \dot{\gamma}^\alpha \boldsymbol{S}_0^\alpha \mathrm{sign}(\tau^\alpha) \tag{4}$$

where $\boldsymbol{S}_0^\alpha = \boldsymbol{m}^\alpha \otimes \boldsymbol{n}^\alpha$ is the Schmid tensor and $\dot{\gamma}^\alpha$ is the plastic shearing rate on the α^{th} slip system. The solution of $\boldsymbol{F}^p$ is computed by assuming a constant shearing rate $\dot{\gamma}^\alpha$ for the time-step:

$$\boldsymbol{F}_{n+1}^p = \exp(\sum_\alpha \Delta\gamma^\alpha \boldsymbol{S}_0^\alpha \mathrm{sign}(\tau^\alpha))\boldsymbol{F}_n^p \tag{5}$$

The term $\dot{\gamma}$ from Eq. 1 changes to $\Delta\gamma$ here, because it is now the increment in infinitesimal time Δt. In Eq. 3, $\boldsymbol{F}^e$ can be obtained as follows:

$$\boldsymbol{F}^e = \boldsymbol{F}_{tr}^e \exp(-\sum_\alpha \Delta\gamma^\alpha \boldsymbol{S}_0^\alpha \mathrm{sign}(\tau^\alpha)) \tag{6}$$

where $\boldsymbol{F}_{tr}^e$ is the trial elastic deformation gradient and is given by $\boldsymbol{F}_{n+1}(\boldsymbol{F}_n^p)^{-1}$. Lagrange strain in relaxed configuration can be written as:

$$\boldsymbol{E}^e \;=\; \frac{1}{2}((\boldsymbol{F}^e)^T\boldsymbol{F}^e - \boldsymbol{I}) \tag{7}$$

Let t denote the current time, Δt an infinitesimal time increment, and $\tau = t + \Delta t$. Then, given $\boldsymbol{F}(t), \boldsymbol{F}(\tau)$, $\boldsymbol{m}_0^\alpha, \boldsymbol{n}_0^\alpha, \boldsymbol{\sigma}(t), \boldsymbol{F}^p(t)$ and $s^\alpha(t)$, $\boldsymbol{F}^p(\tau), s^\alpha(\tau), \sigma(\tau)$ need to be determined. First, deformation gradient and Lagrangian strain are shown as

$$\boldsymbol{F}_{tr}^e(\tau) = \boldsymbol{F}(\tau)\ \boldsymbol{F}^p(t)^{-1} \tag{8}$$

$$\boldsymbol{E}_{tr}^e(\tau) = \frac{1}{2}((\boldsymbol{F}_{tr}^e(\tau))^T\boldsymbol{F}_{tr}^e(\tau) - \boldsymbol{I}) \tag{9}$$

In order to find the resolved shear stress, the conjugate stress measure is then defined by

$$\bar{\boldsymbol{T}} \;=\; \det(\boldsymbol{F}^e)(\boldsymbol{F}^e)^{-1}\boldsymbol{\sigma}(\boldsymbol{F}^e)^{-T} \tag{10}$$

while $\bar{\boldsymbol{T}}(\tau)$ is expressed as

$$\bar{\boldsymbol{T}}(\tau) \;=\; \boldsymbol{\mathcal{L}}^e \left[\bar{\boldsymbol{E}}^e(\tau)\right] \tag{11}$$

where $\bar{\boldsymbol{T}}_{tr}(\tau)$ is calculated in the same manner as $\boldsymbol{\mathcal{L}}^e \left[\bar{\boldsymbol{E}}^e{}_{tr}(\tau)\right]$, where $\boldsymbol{\mathcal{L}}^e$ is the fourth-order anisotropic elasticity tensor. The resolved shear stress is given by

$$\tau^\alpha = (\boldsymbol{C}^e(\tau)\bar{\boldsymbol{T}}(\tau)) \cdot \boldsymbol{S}_0^\alpha \tag{12}$$

while the trial resolved shear stress is defined in the same way as $\tau_{tr}^\alpha(\tau) = (\boldsymbol{C}_{tr}^e(\tau)\bar{\boldsymbol{T}}_{tr}(\tau))\cdot\boldsymbol{S}_0^\alpha$. In crystal plasticity theory, the hardening law for the slip resistance s^α at time τ is given as:

$$s^\alpha(\tau) = s^\alpha(t) + \sum_\beta h^{\alpha\beta}(t)\Delta\gamma^\beta \tag{13}$$

where $h^{\alpha\beta}$ describes the rate of increase of the deformation resistance on slip system α due to shearing on slip system β. Now we can determine $\Delta\gamma$ using the equality $|\tau^\alpha| = s^\alpha$, with $\alpha, \beta \in \mathcal{A}$, the active set of slip systems:

$$\sum_{\beta\in\mathcal{A}} A^{\alpha\beta}\Delta\gamma^\beta = b^\alpha \tag{14}$$

where,

$$\begin{aligned} &A^{\alpha\beta} = h^{\alpha\beta}(t) + \text{sign}(\tau_{tr}^\alpha(\tau))\text{sign}(\tau_{tr}^\beta(\tau))(\boldsymbol{C}_{tr}^e(\tau)\boldsymbol{\mathcal{L}}^e\left[\boldsymbol{B}^\beta\right] + 2\boldsymbol{B}^\beta\bar{\boldsymbol{T}}_{tr}(\tau)) \cdot \boldsymbol{S}_0^\alpha, \\ &b^\alpha = |\tau_{tr}^\alpha(\tau)| - s^\alpha(t) > 0, \\ &\Delta\gamma^\beta > 0 \end{aligned} \tag{15}$$

$\boldsymbol{B^\beta} = \frac{1}{2}((\boldsymbol{S}_0^\beta)^T(\boldsymbol{F}_{tr}^e)^T\boldsymbol{F}_{tr}^e + (\boldsymbol{F}_{tr}^e)^T\boldsymbol{F}_{tr}^e\boldsymbol{S}_0^\beta)$

Eq. 14 is a system of linear equations. However, the elements of the set $\mathcal{A}$ are not known. They are determined in an iterative fashion. It is initially assumed that all the potentially active systems are active

$$\sum_{\beta\in\mathcal{PA}} A^{\alpha\beta}\Delta\gamma^\beta = b^\alpha \tag{16}$$

and this linear system is solved. We look for elements with $\Delta\gamma^\beta > 0$, the systems with $\Delta\gamma^\beta \leqslant 0$ are considered inactive and are removed from the list of active slip systems. The reduced system is solved and the procedure is repeated until all $\Delta\gamma^\beta > 0$. Only values of $\Delta\gamma$ larger than 0 are kept.

Then, $\boldsymbol{F}^p(\tau)$ can be updated by Eq. 5, $\boldsymbol{F}^e(\tau)$ updates through Eq. 3 or Eq. 6. In order to update $\boldsymbol{\sigma}(\tau)$, $\bar{\boldsymbol{T}}(\tau)$ needs to be updated first, Eq. 11. Then $\boldsymbol{\sigma}(\tau)$ can be found by $\boldsymbol{\sigma}(\tau) = \boldsymbol{F}^e(\tau)(\det(\boldsymbol{F}^e(\tau)))^{-1}\bar{\boldsymbol{T}}(\tau)\boldsymbol{F}^e(\tau)^T$ from Eq .10, and $s^\alpha(\tau)_i$ can be specified by Eq.13. Once $\boldsymbol{F}^p(\tau)$ and $s^\alpha(\tau)_i$ are updated, we use Eqns. 8 -12 to update the trial resolved shear stresses $\tau_{tr}^\alpha(\tau)_i$. Now, these potentially active systems may not lie on the new yield surface, so we correct for the non-linear model as follows

$$\sum_{\beta\in\mathcal{A}} A^{\alpha\beta}\delta(\Delta\gamma^\beta) = b_i^\alpha \tag{17}$$

Eq. (17) is solved repeatedly only for the initial active slip systems with $b_i^\alpha = |\tau^\alpha(\tau)|_i - s^\alpha(\tau)_i$ and $A^{\alpha\beta} = h^{\alpha\beta}(t) + \text{sign}(\tau_{tr}^\alpha(\tau))\text{sign}(\tau_{tr}^\beta(\tau))(\boldsymbol{C}_{tr}^e(\tau)\boldsymbol{\mathcal{L}}^e\left[\boldsymbol{B}^\beta\right] + \boldsymbol{B}^\beta\bar{\boldsymbol{T}}_{tr}(\tau)) \cdot \boldsymbol{S}_0^\alpha$ and $\Delta\gamma^\beta$ is updated and used to compute until $\boldsymbol{F}^p(\tau)$, $\tau_{tr}^\alpha(\tau)_i$ and $s^\alpha(\tau)_i$ until $b_i^\alpha < \epsilon$ is reached. Here ϵ is the specified stress tolerance and i is the iterative step. If ϵ is set high, it is equivalent to doing one iteration, which is similar to [2].

Once $\boldsymbol{F}^p(\tau)$ and $s^\alpha(\tau)$ are updated, we use Eqns. (8 -12) to update the trial resolved shear stresses $\tau_{tr}^\alpha(\tau)$ for all the other slip systems. If for some of the slip systems $|\tau_{tr}^\alpha(\tau)| > s^\alpha(\tau)+\epsilon$, then the procedure is repeated from 14 to ensure that all the slip systems lie on or inside the new yield surface.

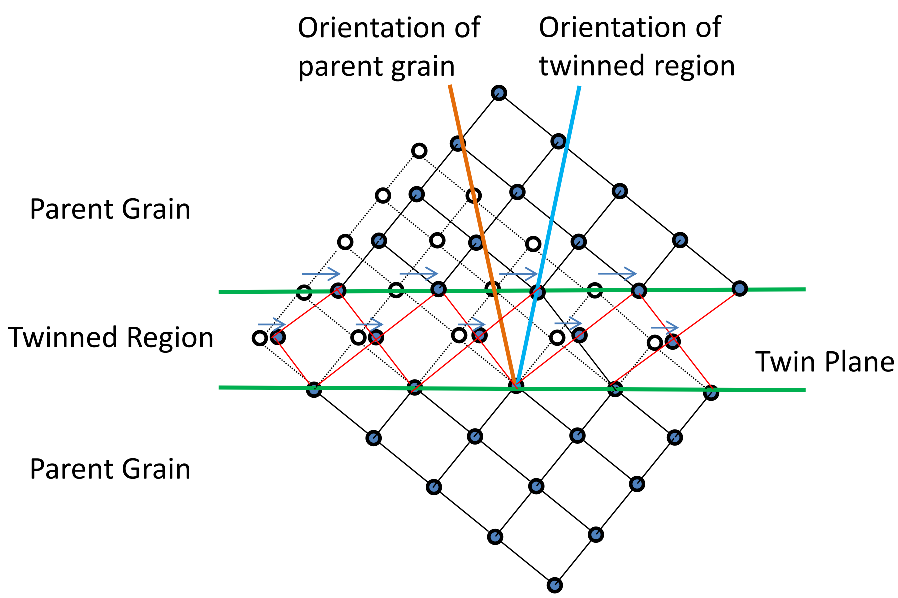

Figure 3: Crystallography of twinned region

Modeling Deformation Twinning in HCP Alloys

The crystallography of twins is shown in Fig. 3 indicating the parent grain, twinned region and the orientation of the corresponding regions. The kinematics of slip and twinning is shown in Fig. 4. Twin systems are initially considered as slip systems and are sheared until they are reoriented. Our formulation for twinning closely follows the approach adopted by Staroselsky et al.[3] . The differences in the approach are as follows :

1) We adopt the Predominant Twin Reorientation scheme (PTR) [4] instead of the scheme proposed by Van Houtte [5] . As more elements are reoriented, the PTR scheme inhibits further reorientation by twinning until accumulated fraction catches up as the deformation

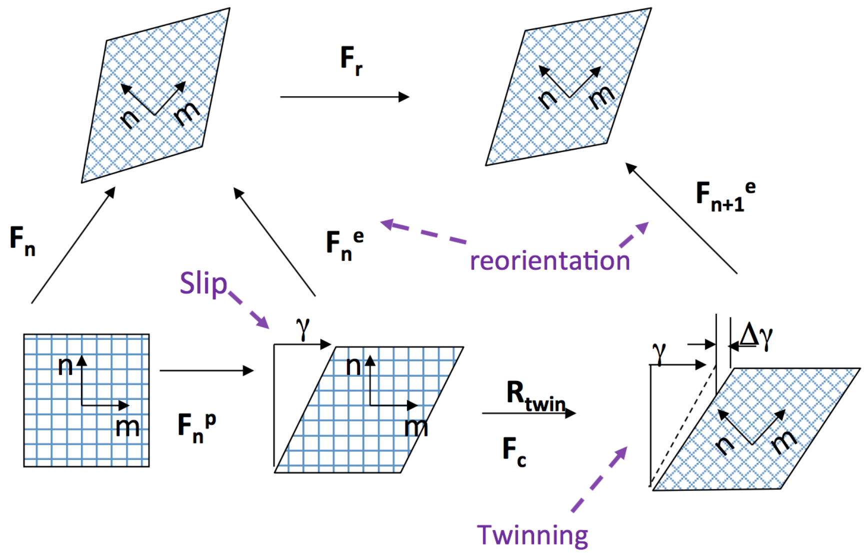

Figure 4: Kinematics of slip and twinning

proceeds.

2) The individual quadrature points are reoriented as compared to reorienting the entire grain. We keep track of the orientations of all quadrature points in the FE simulation and reorient the individual points which satisfy the PTR scheme[4]. The approach in [3] considers each grain as represented by a single element whereas in the current approach each grain is represented by multiple elements.

3) We use Implicit FEM which enforces static equilibrium at each time step compared to Explicit FEM used by Staroselsky et al.

Reorientation Scheme

Fraction of the grain associated with each twinning system is given by

$$g^{n,t_i} = \Sigma_{steps} \Delta g^{n,t_i} \tag{18}$$

where $g^{n,t_i} = \frac{\Delta \gamma^{n,t_i}}{S}$, n is the n^{th} quadrature point, steps is the number of time-steps, t_i is the i^{th} twinning system and S is the characteristic twin shear strain.

Threshold fraction for twinning is calculated locally at each element making the method locally-sensitive

$$F_T = 0.25(1 + \frac{N}{\Sigma_i g^{n,t_i}}) \tag{19}$$

where N is total reoriented volume fraction of the grain. If $g^{n,t_i} > F_T$, the quadrature point is reoriented due to twinning.

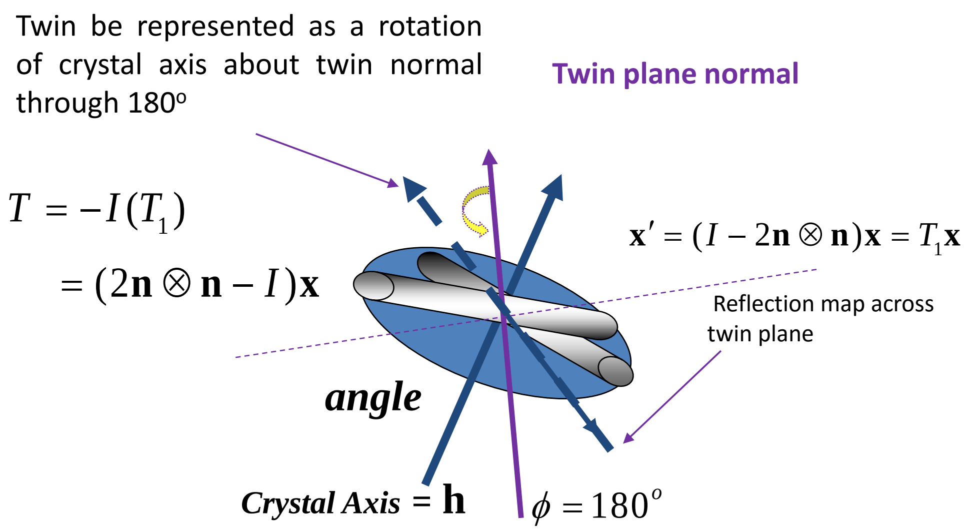

Figure 5: Reorientation due to twinning

Lattice Reorientation Due To Twinning

A schematic diagram of reorientation due to twinning is shown in Fig. 5. The procedure to find the new orientation for the reoriented grain,

1) Find the rotation matrix for reference frame to crystal frame, $\boldsymbol{R_1}$
2) Find the rotation matrix for rotating the crystal frame about the twin plane by 180^o , $\boldsymbol{R_2}$
3)New rotation matrix $\boldsymbol{Q} = \boldsymbol{R_1} \cdot \boldsymbol{R_2}$.
4)Project $\boldsymbol{Q}$ to the fundamental region (QF) based on crystal symmetries.
5) Convert the rotation matrix QF to Rodrigues vector.s
The plastic component of the deformation gradient is updated in the crystal frame to accommodate the reorientation due to twinning. The rotation matrix for rotating the crystal frame about the twin plane $\boldsymbol{R_2}$ is given by

$$\boldsymbol{R_2} = 2\boldsymbol{n_i} \otimes \boldsymbol{n_i} - \boldsymbol{I} \tag{20}$$

Tangent Modulus

The kinematic problem can be expressed in Lagrangian framework as

$$\nabla_0 \cdot \boldsymbol{P} + \boldsymbol{f} = \boldsymbol{0} \tag{21}$$

where ∇_0 is the divergence in the initial reference configuration, $\boldsymbol{P}$ is the polycrystal Piola-Kirchhoff-I stress and $\boldsymbol{f}$ is the reference body force.

$$\boldsymbol{P} = \det(\boldsymbol{F})\boldsymbol{\sigma}\boldsymbol{F}^{-T} \tag{22}$$

Principle of virtual work states that $\mathcal{B}_0$ is in equilibrium if and only if the Piola-Kirchoff stress field, $\boldsymbol{P}$, satisfies the virtual work functional for any kinematically admissible test function $\tilde{\boldsymbol{u}}$,

$$\mathcal{G}(\boldsymbol{u}, \tilde{\boldsymbol{u}}) \equiv \int_{\mathcal{B}_0} \boldsymbol{P} \cdot \nabla_0 \tilde{\boldsymbol{u}} dV - \int_{\partial\mathcal{B}_0} \boldsymbol{\lambda} \cdot \tilde{\boldsymbol{u}} dA - \int_{\mathcal{B}_0} \boldsymbol{f} \cdot \tilde{\boldsymbol{u}} dV = 0 \qquad \forall \tilde{\boldsymbol{u}} \in \mathcal{V} \tag{23}$$

where $\boldsymbol{u}$ is the displacement field, $\mathcal{V}$ is a finite dimensional vector space of all admissible shape functions in the material domain, where $\boldsymbol{f}$ and $\boldsymbol{\lambda}$ denote, respectively, the reference body force and surface traction field.

The dependence of $\mathcal{G}$ on the unknown function $\boldsymbol{u}$ follows from the constitutive dependence of the stress tensor on the strain tensor which, in turn depends on the field $\boldsymbol{u}$. In the above, $\boldsymbol{P}$ is a function of the displacement field due to its constitutive dependence on the deformation gradient $\boldsymbol{F} = \boldsymbol{I} + \nabla_0 \boldsymbol{u}$.

Newton-Raphson iterative scheme with a line search procedure is employed. The Gâteaux derivative of $\mathcal{G}$ at $\boldsymbol{u}_n$ in the direction of $\Delta\boldsymbol{u}$ is given by

$$\frac{\partial \mathcal{G}(\boldsymbol{u}_n, \tilde{\boldsymbol{u}})}{\partial \boldsymbol{u}_n} \Delta\boldsymbol{u} = \int_{\mathcal{B}_0} \boldsymbol{A} \frac{\partial \boldsymbol{F}}{\partial \boldsymbol{u}_n} \cdot \nabla_0 \tilde{\boldsymbol{u}} dV \Delta\boldsymbol{u} \tag{24}$$

where

$$\boldsymbol{A} \equiv \left. \frac{\partial \boldsymbol{P}}{\partial \boldsymbol{F}} \right|_{\boldsymbol{F}_n} \tag{25}$$

is generally termed the material tangent modulus.

The Piola-Kirchhoff-I stress, shown as $\boldsymbol{P}$ can be expanded as

$$\begin{aligned} \boldsymbol{P} &= \det(\boldsymbol{F})\boldsymbol{\sigma}\boldsymbol{F}^{-T} \\ &= \det(\boldsymbol{F})((det(\boldsymbol{F}^e))^{-1}\boldsymbol{F}^e\bar{\boldsymbol{T}}(\boldsymbol{F}^e)^T)\boldsymbol{F}^{-T} \\ &= \boldsymbol{F}^e\bar{\boldsymbol{T}}(\boldsymbol{F}^e)^T\boldsymbol{F}^{-T} \quad (\quad \det(\boldsymbol{F}) = \det(\boldsymbol{F}^e).) \end{aligned} \tag{26}$$

The variation of PKI stress at time τ is given by

$$\begin{aligned} \delta\boldsymbol{P} &= \delta(\boldsymbol{F}^e\bar{\boldsymbol{T}}(\boldsymbol{F}^e)^T\boldsymbol{F}^{-T}) \\ &= \delta(\boldsymbol{F}^e)\bar{\boldsymbol{T}}(\boldsymbol{F}^e)^T\boldsymbol{F}^{-T} + \boldsymbol{F}^e\delta(\bar{\boldsymbol{T}})(\boldsymbol{F}^e)^T\boldsymbol{F}^{-T} + \boldsymbol{F}^e\bar{\boldsymbol{T}}\delta((\boldsymbol{F}^e)^T)\boldsymbol{F}^{-T} \\ &\quad + \boldsymbol{F}^e\bar{\boldsymbol{T}}(\boldsymbol{F}^e)^T\delta(\boldsymbol{F}^{-T}) \\ &= \delta(\boldsymbol{F}^e)\bar{\boldsymbol{T}}(\boldsymbol{F}^e)^T\boldsymbol{F}^{-T} + \boldsymbol{F}^e\delta(\bar{\boldsymbol{T}})(\boldsymbol{F}^e)^T\boldsymbol{F}^{-T} + \boldsymbol{F}^e\bar{\boldsymbol{T}}(\delta\boldsymbol{F}^e)^T\boldsymbol{F}^{-T} \\ &\quad + \boldsymbol{F}^e\bar{\boldsymbol{T}}(\boldsymbol{F}^e)^T\delta(\boldsymbol{F}^{-1})^T \\ &= \delta(\boldsymbol{F}^e)\bar{\boldsymbol{T}}(\boldsymbol{F}^e)^T\boldsymbol{F}^{-T} + \boldsymbol{F}^e\delta\bar{\boldsymbol{T}}(\boldsymbol{F}^e)^T\boldsymbol{F}^{-T} + \boldsymbol{F}^e\bar{\boldsymbol{T}}(\delta\boldsymbol{F}^e)^T\boldsymbol{F}^{-T} \\ &\quad - \boldsymbol{F}^e\bar{\boldsymbol{T}}(\boldsymbol{F}^e)^T(\boldsymbol{F}^{-1})^T\delta(\boldsymbol{F})^T(\boldsymbol{F}^{-1})^T \end{aligned} \tag{27}$$

where $\delta \boldsymbol{F}^e$ is obtained as:

$$\begin{aligned}\delta(\boldsymbol{F}^e) &= \delta \boldsymbol{F}(\boldsymbol{F}^p)^{-1} + \boldsymbol{F}\delta((\boldsymbol{F}^p)^{-1}) \\ &= \delta \boldsymbol{F}(\boldsymbol{F}^p)^{-1} - \boldsymbol{F}(\boldsymbol{F}^p)^{-1}\delta \boldsymbol{F}^p(\boldsymbol{F}^p)^{-1}\end{aligned} \tag{28}$$

Then the computation of $\delta\bar{\boldsymbol{T}}$ can be obtained as from Eq. 11,

$$\delta\bar{\boldsymbol{T}} \quad = \quad \boldsymbol{\mathcal{L}}^e\left[\delta\bar{\boldsymbol{E}}^e\right] \tag{29}$$

while

$$\delta\bar{\boldsymbol{E}}^e \quad = \quad \frac{1}{2}((\delta \boldsymbol{F}^e)^T\boldsymbol{F}^e + (\boldsymbol{F}^e)^T\delta(\boldsymbol{F}^e)) \tag{30}$$

The variation of plastic deformation gradient, $\delta(\boldsymbol{F}^p)$ is computed in an iterative manner as follows

$\delta \boldsymbol{F}^e_{tr}$ is obtained as:

$$\begin{aligned}\delta(\boldsymbol{F}^e_{tr_i}) &= \delta \boldsymbol{F}(\boldsymbol{F}^p_{i-1})^{-1} + \boldsymbol{F}\delta((\boldsymbol{F}^p_{i-1})^{-1}) \\ &= \delta \boldsymbol{F}(\boldsymbol{F}^p_{i-1})^{-1} - \boldsymbol{F}(\boldsymbol{F}^p_{i-1})^{-1}\delta(\boldsymbol{F}^p_{i-1})(\boldsymbol{F}^p_{i-1})^{-1}\end{aligned} \tag{31}$$

where $\boldsymbol{F}^p_i$ is the plastic deformation gradient in the i^{th} active set search completed to include the slip systems lying outside the yield surface. Before the beginning of active set search, $\boldsymbol{F}^p_0 = \boldsymbol{F}^p_n$ and $\delta\boldsymbol{F}^p_0 = \boldsymbol{0}$, where $\boldsymbol{F}^p_n$ is the plastic deformation gradient from the previous time-step.

$$\delta\bar{\boldsymbol{E}}^e{}_{tr_i} = \frac{1}{2}((\delta \boldsymbol{F}^{\boldsymbol{e}}{}_{tr_i})^T\boldsymbol{F}^e + (\boldsymbol{F}^e)^T\delta(\boldsymbol{F}^e_{tr_i})) \tag{32}$$

$$\delta\bar{\boldsymbol{T}}_{tr_i} \quad = \quad \boldsymbol{\mathcal{L}}^e\left[\delta\bar{\boldsymbol{E}}^e{}_{tr_i}\right] \tag{33}$$

$\delta(\Delta\gamma^\beta)$ in this equation is evaluated as following:

$$\begin{aligned}\delta b^\alpha_i &= \operatorname{sign}(\tau^\alpha_{tr_i})\delta(\boldsymbol{C}^e_{tr_i}\bar{\boldsymbol{T}}_{tr_i})\cdot\boldsymbol{S}^\alpha_0 - \delta(s^\alpha_{i-1}) \\ &= \operatorname{sign}(\tau^\alpha_{tr_i})(\delta(\boldsymbol{C}^e_{tr_i})\bar{\boldsymbol{T}}_{tr_i} + \boldsymbol{C}^e_{tr_i}\delta(\bar{\boldsymbol{T}}_{tr_i}))\cdot\boldsymbol{S}^\alpha_0 - \delta(s^\alpha_{i-1}) \\ &= \operatorname{sign}(\tau^\alpha_{tr_i})(2\delta(\bar{\boldsymbol{E}}^e{}_{tr_i})\bar{\boldsymbol{T}}_{tr_i} + \boldsymbol{C}^e_{tr_i}\delta(\bar{\boldsymbol{T}}_{tr_i}))\cdot\boldsymbol{S}^\alpha_0 - \delta(s^\alpha_{i-1})\end{aligned} \tag{34}$$

The variation of slip system resistance s^α is computed as follows

$$\begin{aligned}\delta(s^\alpha_i) &= \delta(s^\alpha_{i-1}) + \sum_\beta \delta h^{\alpha\beta}_i\Delta\gamma^\beta + \sum_\beta h^{\alpha\beta}_i\delta(\Delta\gamma^\beta) \\ &= \delta(s^\alpha_{i-1}) + \sum_\beta h^{\alpha\beta}_i\delta\Delta\gamma^\beta \\ &\quad + \sum_\beta h^\beta_o(q + (1-q)\delta^{\alpha\beta})\left(1 - \frac{s^\beta_i}{s^\beta_s}\right)^{(a-1)}\left(\frac{-1}{s^\beta_s}\right)\delta(s^\beta_{i-1})\Delta\gamma^\beta\end{aligned} \tag{35}$$

The variation of slip shear increment $\delta(\Delta\gamma^\beta_i)$ is therefore

$$\delta(\Delta\gamma_i^\beta) = (A_i^{\alpha\beta})^{-1}(\delta b_i^\alpha - \delta A_i^{\alpha\beta}\Delta\gamma_i^\beta) \tag{36}$$

$$\delta A_i^{\alpha\beta} = \delta h_i^{\alpha\beta} + \text{sign}(\tau_{tr}^\alpha(\tau))\text{sign}(\tau_{tr}^\beta(\tau))(\delta \boldsymbol{C}_{tr_i}^e(\tau)\boldsymbol{\mathcal{L}}^e\left[\boldsymbol{B}_i^\beta\right] + \boldsymbol{C}_{tr_i}^e(\tau)\boldsymbol{\mathcal{L}}^e\left[\delta\boldsymbol{B}_i^\beta\right] + 2\delta\boldsymbol{B}_i^\beta\bar{\boldsymbol{T}}_{tr_i}(\tau) + 2\boldsymbol{B}_i^\beta\delta\bar{\boldsymbol{T}}_{tr_i}(\tau))\cdot\boldsymbol{S}_0^\alpha \tag{37}$$

while, $\delta\boldsymbol{B_i^\beta} = 0.5((\boldsymbol{S}_0^\beta)^T\delta\bar{\boldsymbol{E}}_{tr_i}^e + \delta\bar{\boldsymbol{E}}_{tr_i}^e\boldsymbol{S}_0^\beta)$ and $\delta h_i^{\alpha\beta} = h_o^\beta(q+(1-q)\delta^{\alpha\beta})\left(1-\frac{s_i^\beta}{s_s^\beta}\right)^{(a-1)}\left(\frac{-1}{s_s^\beta}\right)\delta(s_{i-1}^\beta)$

$\boldsymbol{F}^p$ is updated as follows :

$$\delta(\boldsymbol{F}_i^p) = \delta(\exp(\textstyle\sum_\alpha \Delta\gamma_i{}^\alpha\boldsymbol{S}_0^\alpha\text{sign}(\tau^\alpha)))(\boldsymbol{F}_{i-1}^p) + \exp(\textstyle\sum_\alpha \Delta\gamma_i{}^\alpha\boldsymbol{S}_0^\alpha\text{sign}(\tau^\alpha))\delta(\boldsymbol{F}_{i-1}^p) \tag{38}$$

References

[1] Anand, L. (1985), Constitutive equations for hot-working of metals, International Journal of Plasticity, 1 (3), 213-231.
[2] Anand, L., and M. Kothari. ”A computational procedure for rate-independent crystal plasticity.” Journal of the Mechanics and Physics of Solids 44.4 (1996): 525-558.
[3]Staroselsky, A., and L. Anand (2003), A constitutive model for hcp materials deforming by slip and twinning: application to magnesium alloy az31b, International journal of Plasticity, 19 (10), 1843-1864
[4] Tome, C. N., R. A. Lebensohn, and U. F. Kocks. ”A model for texture development dominated by deformation twinning: application to zirconium alloys.” Acta Metallurgica et Materialia 39.11 (1991): 2667-2680
[5]Van Houtte, P. (1978), Simulation of the rolling and shear texture of brass by the taylor theory adapted for mechanical twinning, Acta Metallurgica, 26 (4), 591-604